energies

Article

Quantification of Dust Accumulation on Solar Panels Using the Contact-Characteristics-Based Discrete Element Method

Shing-Lih Wu [1], Hung-Cheng Chen [2,*] and Kai-Jun Peng [2]

[1] Department of Electrical Engineering, National Taitung Junior College, 911, Jhengci N. Rd., Taitung 95045, Taiwan
[2] Department of Electrical Engineering, National Chin-Yi University of Technology, 57, Section 2, Chungshan Road, Taiping District, Taichung 41107, Taiwan
* Correspondence: hcchen@ncut.edu.tw; Tel.: +886-4-23924505

Abstract: Dust comprises particles usually present in the atmosphere. The deposition of dust on the surface of the solar panel seriously affects the light transmittance, resulting in lower pow-er generation efficiency and shortening the service life of the solar panel. Therefore, it is important to understand the dust distribution on the surface of solar panels and discuss the influence of dust on the power generation efficiency of solar panels for the efficient prevention of dust deposition on the panel. In this study, to analyze the dust distribution on the surface of the solar panel, the discrete element method was used to establish the contact mechanics model between dust particles and the solar panel. The number of dust particles on the surface of solar panels was calculated at different solar panel inclination angles, wind speeds, and wind directions. The wind speed of 1 and 3 m/s did not affect the dust deposition significantly but the speed over 5 m/s reduced the dust particles from the surface of the solar panel. The inclination angle of 23° influenced dust deposition on the surface of the solar panel. Wind direction did not show a significant effect on dust deposition. The longer the deposition time, the more particles remained on the surface due to the increased force between the particles and the surface of the solar panel. The results from calculation and measurement from transmittance were similar with a different rate of 3.41%. Thus, the result of the proposed calculation in this study provides a basis for de-signing the solar power generation plant and decision-making on the maintenance of the solar panel.

Keywords: solar panel; dust distribution; discrete element method; contact characteristics

Citation: Wu, S.-L.; Chen, H.-C.; Peng, K.-J. Quantification of Dust Accumulation on Solar Panels Using the Contact-Characteristics-Based Discrete Element Method. *Energies* **2023**, *16*, 2580. https://doi.org/10.3390/en16062580

Academic Editors: Chun-Yen Chang, Teen-Hang Meen, Charles Tijus, Po-Lei Lee and Jeff Kettle

Received: 2 November 2022
Revised: 29 December 2022
Accepted: 1 March 2023
Published: 9 March 2023

1. Introduction

The increasing demand for energy causes the "energy security crisis" more prominent than before. "Global warming" caused by using fossil fuels also emerges more seriously [1]. Renewable energy source, especially, solar energy is ideal for sustainable development with the advantages of inexhaustibility and easier expansion of generation capacity. Solar energy is an appropriate power source for remote areas and emergency power backup, too. It does not require labor-intensive mining and is environment friendly allowing ecological conservation and suppression of carbon dioxide emission [2,3].

Therefore, researchers have researched solar cells from varius perspectives. With a huge investment, the power generation of solar cells has improved considerably but it still is limited by natural causes such as dust deposition [4–6]. Even in remote areas where solar power plants are built, dust problems are unavoidable as dust is produced from natural sources (wind, volcanic activity, and so on) as well as anthropogenic sources (construction, transportation, and other human activities). Dust deposition on the solar panel is one of the most important factors in managing solar power production [7]. The size, composition, and shape of dust vary a lot as dust may contain pollens, human and animal cells, hairs, textile fibers, and minerals [8]. Dust and other various environmental factors including irradiance, rain, and wind affects solar panel temperature and light transmittance which again influences power production [9]. Especially, the efficiency of solar power production is greatly affected by a layer of dust (usually less than 10 μm) as dust hinders the radiation onto the solar cell. The deposition of dust particles on the surface of the solar panel seriously affects the power generation efficiency of the solar panel, decreasing power generation efficiency and shortening the service life of the solar panel.

Hertz [10] proposed the theory of contact related to the static interaction of particles. He found a relationship between the contact area and elastic deformation between particles. Recently, research on the adhesion of dust particles to the surface has been conducted based on his theory. Cundall and Strack [11] proposed the concept of the soft sphere model to describe the adhesion between microscopic particles and proposed the discrete simulation analysis of the particulate matter numerically.

To analyze the distribution of dust on the surface of solar panels over time and explore its influence on the efficiency of power generation, we established a contact model with the discrete element method to explain the interaction between dust particles and solar panels, considering the inclination angles of the solar panel, wind speed, and direction, the distribution of dust on the surface of solar panels. In the research, it was assumed that the surface of the solar panel was exposed to the atmosphere and received dust particles falling from the air. For modeling, a micro weather station and an automatic dust measurement platform were designed and installed. The atmospheric parameters and the dust deposition on the surface were measured to verify the accuracy of the proposed model and compare the simulation results to the measured distribution of dust particles. The result provides the basic information for the design of the solar power plant and the maintenance of the solar panel.

2. Contact Mechanism Model Based on the Discrete Element Method

The discrete element method was proposed by Cundall based on the principle of molecular dynamics for the analysis of discrete particle behavior [12]. The discrete element method was analogous to the process of motion of particles spreading in the air. The motion of particles inevitably causes collisions and generates various forces between particles. The process of the collision described by the discrete element method describes the basic process of contact generation and the following motions of particles.

To quantify the impact of dust deposition on solar panel power generation, a model was established to evaluate the impact based on the data on the amount of dust and wind intensity. For the model, the contact mechanism model was adopted with the following assumptions.

(1) The distribution of dust particles was uniform in the surrounding environment of the solar panel. The particle shape was spherical and the particle sizes were randomly distributed. A friction coefficient was used to compensate for the error caused by the irregular shapes of dust particles.
(2) Gravity and van der Waals forces were considered between dust particles.

Based on the above two assumptions, the physical parameters of the contact between dust particles and solar panels were named as shown in Table 1 [13].

Table 1. Parameters for two spherical particles.

	Dust Particles 1	**Dust Particles 2 or Solar Panels**
Radius	R_1	R_2
Sphere Center Position Vector	r_1	r_2
Elastic Modulus	E_1	E_2
Poisson's Ratio	γ_1	γ_2
Quality	m_1	m_2
Pre-Collision Velocity Vector	v_1	v_2
Shear Modulus	G_1	G_2

The normal force F_n between dust particles or between the particles and the solar panel is expressed as follows [13].

$$F_n = -4\sqrt{\pi\gamma E^* \alpha^3} + \frac{4E^* \alpha^3}{3R^*} \quad (1)$$

where γ is the surface energy of solar energy, E^* is the comprehensive elastic modulus, R^* is the comprehensive radius of particles, and α is the normal overlap.

The tangential force F_t between dust particles or between the particles and the solar panel is expressed as Equation (2) [13].

$$F_t = -S_t \delta \quad (2)$$

where S_t is the tangential stiffness and δ is the tangential overlap.

The S_t tangential stiffness is expressed as the following equation [13].

$$S_t = 8G^* \sqrt{R^* \alpha} \quad (3)$$

where G^* is the equivalent shear modulus, R^* is the comprehensive radius of the particle, and α is the normal overlap amount.

The friction force f between dust particles or between the particles and the solar panel is expressed as Equation (4) [13].

$$f = \mu_s F_n \quad (4)$$

where F_n is the normal force and μ_s is the static friction coefficient.

The rolling friction is extremely important in the analysis. The rolling friction is calculated by the moment T_i between the dust particles or the contact surface between the dust particles and the solar panel, which is expressed as the following equation [13].

$$T_i = -\mu_r F_n R_i \omega_i \quad (5)$$

where μ_r is the coefficient of rolling friction, ω_i is the angular velocity of particle *i* at the point of contact, and R_i is the distance from the center of mass of particle *i* to the contact point.

3. Solar Panel Dust Accumulation Experiment

3.1. Parameters and Equations

Figure 1 shows the simulation model of solar panel dust accumulation, and the particle factory above simulated the falling surface of dust particles. The size of the solar panel glass in the model was 375 × 340 mm, which is the standard size for commercial use. The width of the aluminum alloy frame was 20 mm. The material for the surface of the solar panel was glass.

The physical parameters of the glass panel of the solar panel surface, aluminum alloy frame, and dust particles for simulation are shown in Table 2. Table 3 presents the characteristic parameters of contacts between dust particles and between the particles and the glass or frame (aluminum allow) of the solar panel [13].

Table 2. Solar panel and dust physical parameters.

Parameter	Glass	Aluminum Alloy	Dust Particle
Poisson's Ratio	0.23	0.3897	0.4
Shear Modulus/Pa	2.8×10^{10}	2.7×10^{10}	2×10^{6}
Density/(kg/m^3)	2458	2700	1400

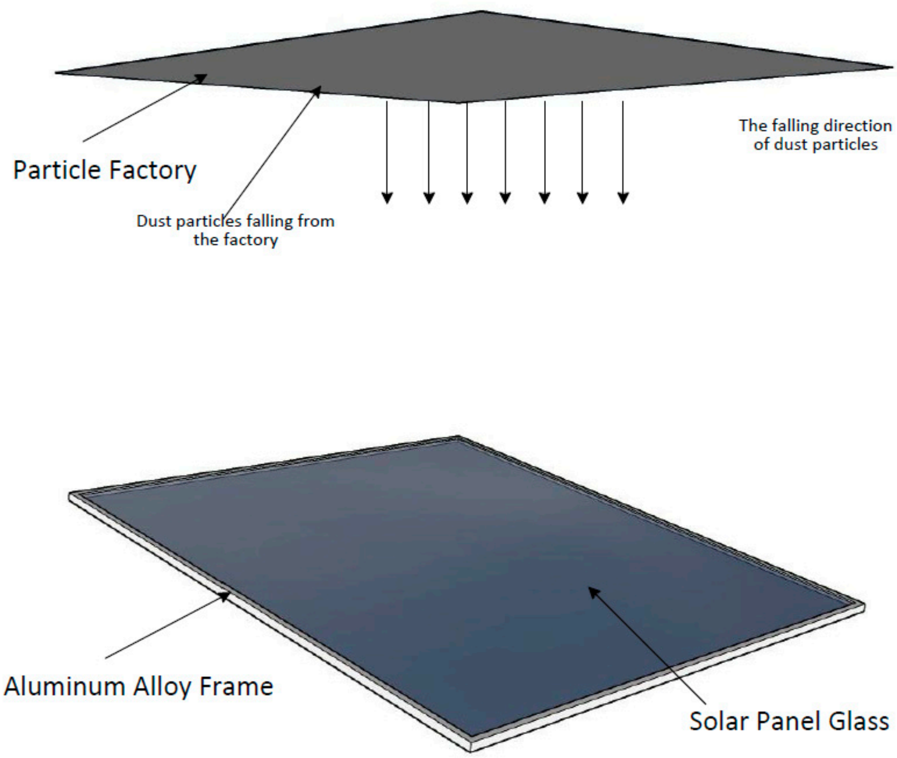

Figure 1. Dust accumulation on a solar panel.

Table 3. Collision characteristic parameters.

Parameter	Dust Particle-to-Particle Contact Coefficient	Coefficient of Contact between Dust Particles and Glass	Coefficient of Contact between Dust Particles and Aluminum Alloys
Coefficient of Recovery	0.5	0.4	0.4
Static Friction Coefficient	0.5	0.7	0.7
Rolling Friction Coefficient	0.1	0.5	0.5

According to the data provided by the automatic dust measurement system in Taichung City (installed and managed by the Environmental Protection Agency of Taiwan), the flux of atmospheric dust on the surface was estimated as 2.29 tons/km^2·month [14]. It was equivalent to 8.834×10^{-16} kg/mm^2·s. For the size of 375 × 340 mm of a solar panel, the flux of the dust on the panel was estimated to be 1.1264×10^{-10} kg/s. To have the amount of 1.1264×10^{-6} kg of dust particles (7951 particles) on the panel, 2.778 h were required. The number of dust particles is calculated based on the density of dust particles on the solar panel, which is 1400 kg/m^3 (Table 2). The volume of a dust particle is 3.0352×10^{-13} m^3 and the mass of a particle is 4.25×10^{-10} kg. As there are three particle factories in the model design, the total mass of dust particles is 1.1264×10^{-10} kg × 3 = 3.3792×10^{-6} kg, so the number of dust particles is calculated as the total mass of dust particles/the mass of a single dust particle (3.3792×10^{-6} kg/4.25×10^{-10} kg) = 7951.

When the flux of dust particles does not change over time, the simulation time can be set as the actual accumulation time (T) for dust deposition on the panel. Thus, the following equation is proposed.

$$T = (T_M \div G_s) \times D_f \quad (6)$$

where T is the actual dust accumulation time on the solar panel, T_M is the total weight of dust, G_s is the area of the solar panel, and D_f is the dust deposition flux in Taichung City.

3.2. Calculation of Dust Deposition

Assuming that dust particles falled on the solar panel surface randomly, we divided the surface into 25 sections. The distribution of dust particles was measured in each section, as shown in Figure 2. For the convenience of analysis, the glass surface was divided into five areas from top to bottom, namely, upper, middle-upper, middle, middle-lower, and lower. Each area contained five sections and the average weight of the dust particles in each area was calculated. After deducting the dust particles on the aluminum alloy, the number of dust particles in each section was calculated.

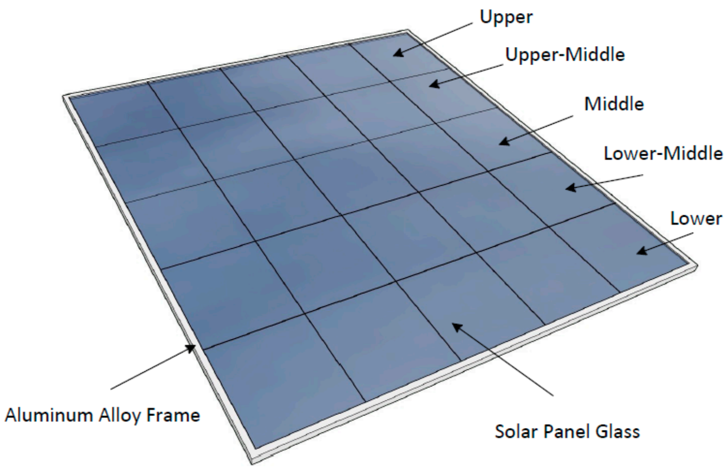

Figure 2. Schematic diagram showing the position of the glass side of the solar panel.

Wind direction and speed data were provided by the Environmental Protection Agency of Taiwan. The location of the actual measurement site was Taichung City, Taiwan. The monthly average wind speed was between 1 and 2 m/s [15].

The inclination angle of the solar panel affects the light absorption of the solar panel dust deposition. In Taiwan (23° N latitude), the inclination angle of solar panels is generally 23°, which gives the maximum solar radiation. Four different inclination angles (10°, 15°, 20°, and 23°) were chosen to compare the dust deposition on the solar panels in simulation. The average wind speed was about 1–2 m/s and the highest wind speed reached about 5–6 m/s in Taichung. To simulate the greatest dust deposition, rain was not considered. In summary, the parameters for simulation in this study included different solar panel inclination angles (10°, 15°, 20°, and 23°), wind speed (1, 3, and 5 m/s), and wind direction (northeast and southwest).

4. Results

4.1. Number of Dust Particles in Each Area

The flux of dust particles varied under different solar panel inclination angles and changed the distribution on the surface of the solar panel regardless of wind direction and speed. In the simulation for 3.5 days, a total of 7951 dust particles were assumed to fall from the particle factory.

Figure 3a depicts the simulation results of particle distribution on the surface of the solar panel at an inclination angle of 10°. A total of 7535 particles were counted on the surface, with 416 not deposited on the solar panel. The dust particles were almost evenly distributed on each section of the surface. The upper area had 50 particles on average less than the middle area. Figure 3b shows the average number of particles over time in five areas (the upper, middle-upper, middle, middle-lower, and lower areas) of the panel. At the inclination angle of 10°, dust particles deposited more on the upper middle and lower middle areas.

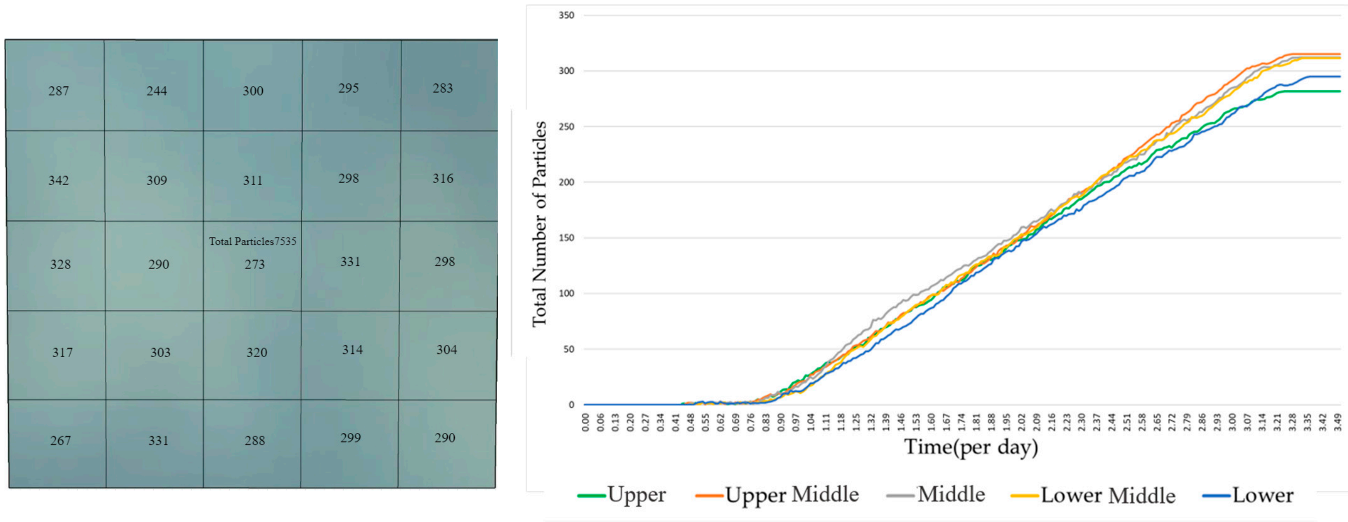

(**a**) (**b**)

Figure 3. Dust particle distribution at an inclination angle of 10°. (**a**) The total number of particles in each area and (**b**) that over time on the solar panel surface.

Figure 4a shows the simulation results of particle distribution on the surface of the solar panel at an inclination angle of 15°. The distribution of dust particles on the surface changed significantly compared to that at the angle of 10°. The particles in the lower areas and the middle area accumulated more than in other areas. The total number of dust particles was 7397, while 554 dust particles did not land on the surface. The number of particles in each area over time was presented in Figure 4b.

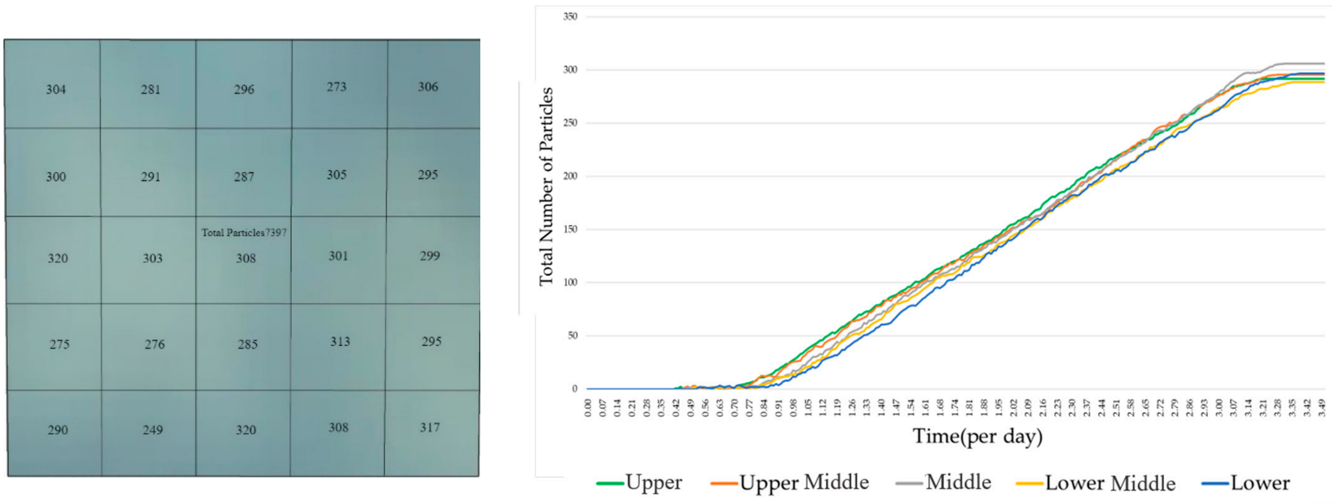

(**a**) (**b**)

Figure 4. Dust particle distribution at an inclination angle of 15°. (**a**) The total number of particles in each area and (**b**) that over time on the solar panel surface.

Figure 5a presents the particle distribution on the surface of the solar panel at an inclination angle of 20°. More dust particles deposited on the upper-middle, middle, and lower-middle areas. There were 7263 dust particles on the glass. Figure 5b shows the number of particles in each area over time.

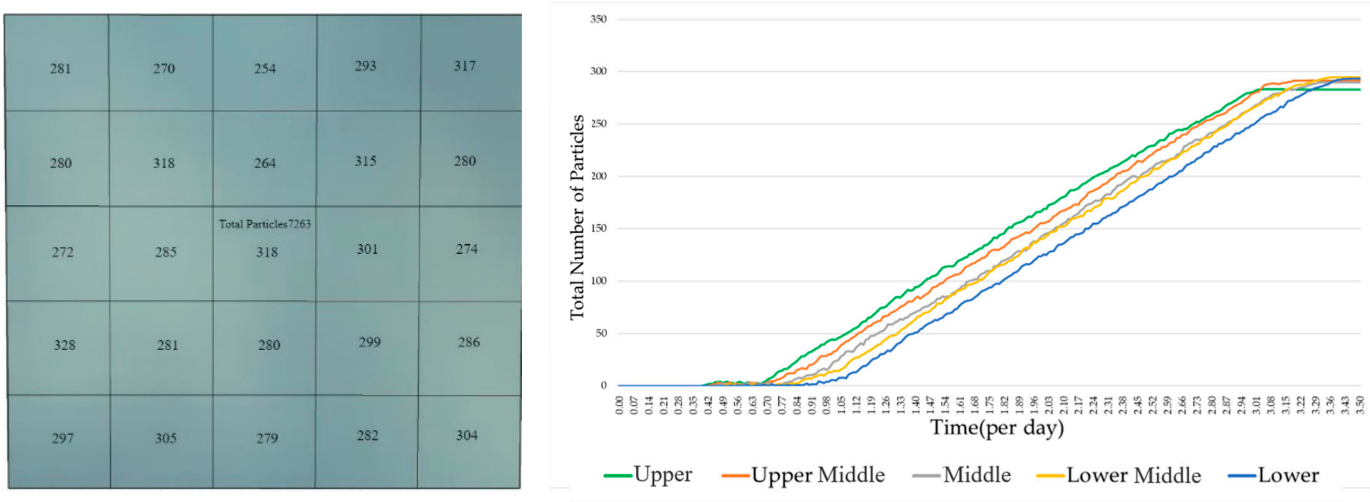

(**a**) (**b**)

Figure 5. Dust particle distribution at an inclination angle of 20°. (**a**) The total number of particles in each area and (**b**) that over time on the solar panel surface.

Figure 6a shows the particle distribution on the surface of the solar panel at an inclination angle of 23°. As the inclination angle increased, dust particles tended to move down from the upper area. Therefore, the upper area had the smallest number of particles. The particles seemed to gather in the upper and lower-middle areas. There were 7065 dust particles on the surface and 886 dust particles were not deposited. More particles were removed at the inclination angle of 23° than at the other angles. Figure 6b presents that more particles were deposited in the other areas than in the upper area. Instead, more particles were deposited on the lower area than at the other inclination degrees.

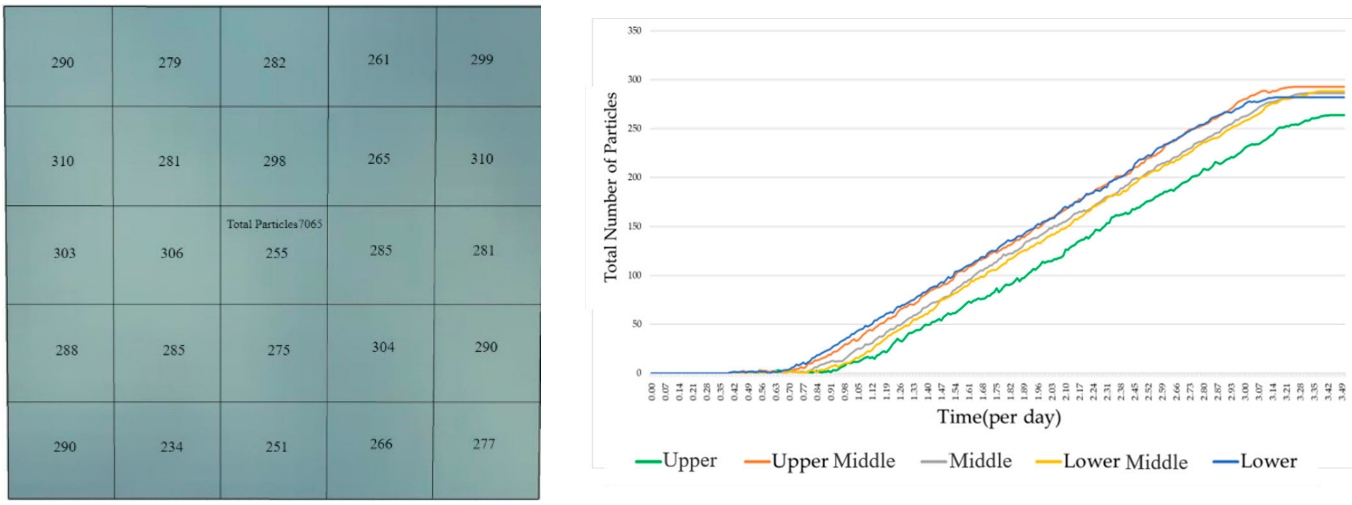

(**a**) (**b**)

Figure 6. Dust particle distribution at an inclination angle of 23°. (**a**) The total number of particles in each area and (**b**) that over time on the solar panel surface.

Table 4 presents the statistics of dust deposition at different inclination angles for 3.5 days. More particles were not deposited with the increase of the inclination angle. The ratio of non-deposited particles to the total number of particles from the particle factory increased accordingly, and the steeper the angle was, the less particles were deposited. The difference in the proportion of non-deposited particles at the inclination angles of 23° and

20° was 2.49%. The differences between the inclination angles of 20° and 15° and between the inclination angles of 15° and 10° were 1.68 and 1.74%.

Table 4. Simulation result of dust deposition for 3.5 days at different inclination angles.

Total Number of Particles / Inclination Angle	Number of Deposited Particles	Number of Non-Deposited Particles	Proportion of Non-Deposited Particles (%)
10°	7535	416	5.23
15°	7397	554	6.97
20°	7263	688	8.65
23°	7065	886	11.14

4.2. Influence of Wind Direction and Speed

The unevenly distributed particles on the surface affected the power generation of the solar panel. The wind blows dust particles, which cleans the surface to a certain extent. The stronger the wind, the more particles are blown away from the surface regardless of wind direction. It was found in this study that the northeast wind removed more dust particles on the surface of the solar panel than the southwest wind at the speed of 5 m/s. Therefore, wind direction rarely affected the dust deposition while wind speed does significantly. The result is shown in Table 5.

Table 5. Simulation result of dust deposition for 3.5 days with the wind at an inclination angle of 10°.

Total Number of Particles / Wind Direction and Speed		Number of Deposited Particles	Number of Non-Deposited Particles	Proportion of Non-Deposited Particles (%)
No Wind		7535	416	5.23
Northeast wind	1 m/s	7467	484	6.09
	3 m/s	7382	569	7.16
	5 m/s	7343	608	7.65
Southwest wind	1 m/s	7515	436	5.48
	3 m/s	7476	475	5.97
	5 m/s	7435	516	6.49

4.3. Dust Deposition for 1 Month

The simulation was carried out for 1 month at an inclination angle of 10° with the wind. The result is shown in Table 6. The proportion of non-deposited particles decreased significantly when compared to that in the simulation for 3.5 days. With no wind, the proportion for 3.5 days was 5.23% while that for 1 month was 3.85%. With the wind, the proportion ranged from 6.09−7.65% in the northeast wind and 5.48−6.49% in the southwest wind for 3.5 days. The proportion in the simulation for 1 month decreased to 4.32−6.27% in the northeast wind and 4.31−4.70% in the southwest wind. The effect of wind direction at the wind speed of 5 m/s became more obvious (6.27% in the northeast wind and 4.70% in the southwest wind). The main reason was that more dust particles were deposited on the surface, which increased the force between the particles and between the particles and the surface of the solar panel, and the force held them on the surface.

Table 6. Simulation result of dust deposition for 1 month with the wind at an inclination angle of 10°.

Wind Direction and Speed / Total Number of Particles		Number of Deposited Particles	Number of Non-Deposited Particles	Proportion of Non-Deposited Particles (%)
No Wind		76,408	3062	3.85
Northeast wind	1 m/s	76,036	3434	4.32
	3 m/s	75,605	3865	4.86
	5 m/s	74,491	4979	6.27
Southwest wind	1 m/s	76,046	3424	4.31
	3 m/s	75,886	3584	4.51
	5 m/s	75,733	3737	4.70

4.4. Dust Deposition for 3 Months

In the simulation for 3 months at an inclination angle of 10° with the wind, the total number of dust particles was 204,961. The proportion of non-deposited particles decreases when compared with that in the simulation of 1 month. In the northeast wind, the proportion in the simulation for 1 month was 4.32–6.27% in the northeast wind and 4.31–4.70% in the southwest wind, while that in the simulation for 3 months was 3.96–5.66% in the northeast wind and 3.63–4.39% in the southwest wind. Without wind, the proportion was similar: 3.99% for 3 months and 3.85% for 1 month. The forces seemed to increase to hold the particles on the surface of the solar panel.

4.5. Particle Deposition Model

In this study, the discrete element method was used to treat the dust particle as multiple discrete units. Ech particle or an aggregate (block) of dust particles is called a unit, and the contact force between units is calculated according to Newton's law of motion. The motion parameters of the unit are calculated to realize the prediction of the motion of the object. As a unit is a particle or an aggregate, the particle model and block method need to be considered for understanding their movements on the surface.

In the particle model, the motion of a particle is independent, and when the particles collide with each other, they interact at the point of contact. The dispersive characteristics of particles produce complex movements under various forces. In practical applications, it is necessary to treat particles as discs and spheres, that is, two-dimensional circular particles and three-dimensional spherical particles. Figure 7 shows the contact between particles (assumed to be spheres) and the contact between particles and surface, where P_n represents a particle. The contact is regarded as a Hertz contact unit including particles and particles and particles and boundaries, where R_1 and R_2 are the contact radii of particles Z_1 and Z_2 respectively, A is the radius of the contact circle, and δ is the deformation of the contact (Figure 8) [16].

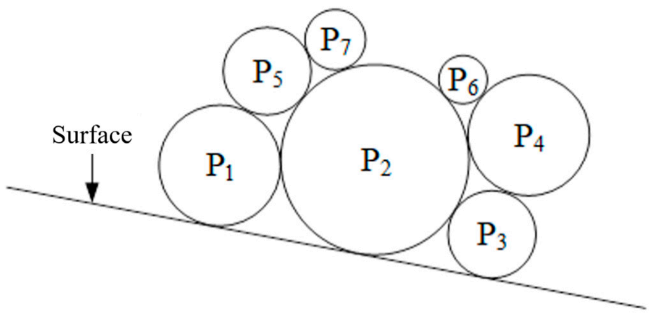

Figure 7. Particle-to-particle contact and particle-to-surface contact.

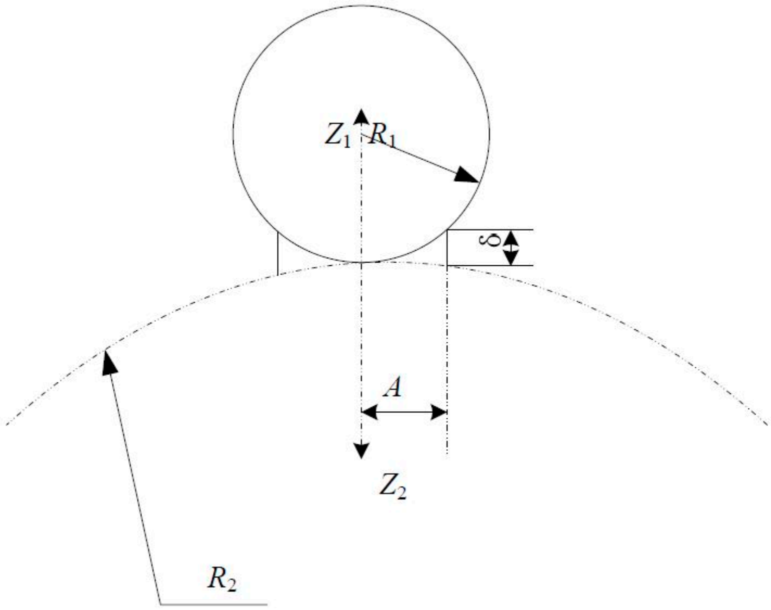

Figure 8. Hertz contact element [16].

In the block model, the main object is an aggregate of particles. At present, the commonly used spherical particle contact mechanism in discrete aggregates is explained by the hard-sphere model and the soft-sphere model to simplify the contact problem [17]. The hard-sphere model does not consider the contact force and contact deformation during the particle contact process, simplifying the entire contact process into a collision that occurs in a very short time. The soft-sphere model is simpler than the hard-sphere model as a simplified contact force is considered between soft-ball particles. The force on particles is described with a damper and spring, and the tangential force is simplified as a damper, sliding machine, and spring.

In this study, we assumed that the aggregation of dust particles followed the hard-sphere model, and the force between particles was assumed to be gravity and Van der Waals force. Therefore, particles and aggregates of particles were affected by such forces, which were related to the different numbers of particles on the surface of the solar panel with different inclination angles of the solar panel.

5. Experiment for Verifying the Calculation Result

To verify the result of the simulation, an automatic dust measurement platform was designed for the experiment. Figures 9 and 10 depict the design and appearance of the platform, in which the inclination angle of the solar panel was fixed at 10°. The platform was exposed to the sun for 3.5 days in the open air and the light transmittance on the surface was measured. The light transmittance was measured with LH-220, a high-precision optical transmittance measuring instrument following "Optical Performance Test Method for Automotive Safety Glass" (the standard of GB5137.2-2002), which is professionally used for glass, heat insulation film, and PVC. Table 7 shows the technical parameters of LH-220 (Table 8). The distribution of dust on the surface of the solar panel was analyzed from the transmittance data. The greater the decrease in transmittance, the more dust that was deposited at the transmittance measurement point. Through the initial measurement of light transmittance, it was confirmed that dust was evenly distributed on the surface. Then, the light transmittance of the solar panel was measured by the platform at nine measurement points. The average value was calculated from the data of the points to obtain the average daylight transmittance.

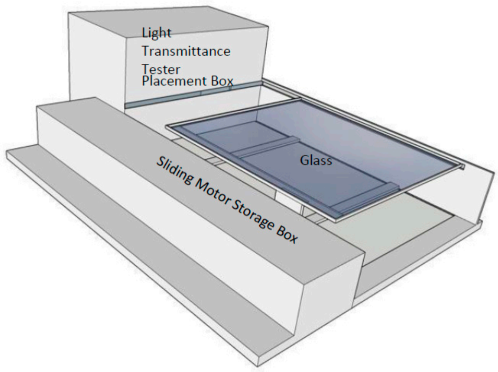

Figure 9. Design of the automatic dust measurement platform.

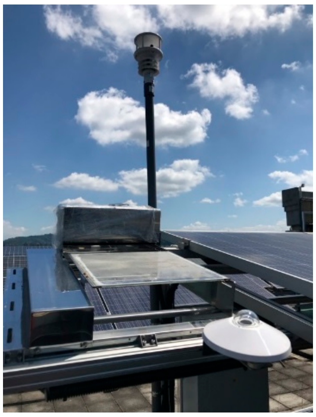

Figure 10. Appearance of the automatic dust measurement platform.

Table 7. Simulation result of dust deposition for 3 months with the wind at an inclination angle of 10°.

Wind Direction and Speed \ Total Number of Particles		Number of Deposited Particles	Number of Non-Deposited Particles	Proportion of Non-Deposited Particles (%)
No Wind		196,775	8186	3.99
Northeast wind	1 m/s	196,838	8123	3.96
	3 m/s	195,258	9703	4.73
	5 m/s	193,365	11,596	5.66
Southwest wind	1 m/s	197,530	7431	3.63
	3 m/s	197,368	7593	3.70
	5 m/s	195,971	8990	4.39

Table 8. Measurement parameters of LH-220.

Wavelength of light source	380–760 nm
Measurement range	0–100%
Resolution	0.1%
Measurement error	≤1%
Thickness for measurement	≤50 mm

First, the light transmittance of the solar panel was measured. There were 25 measurement points in each section. Figure 11 shows an example of the measured light transmittance at each point. It was observed that dust was evenly distributed on the surface, with similar transmittance of 86–88%. When the surface was clean, the light transmittance was 94%. Taking 94% of the light transmittance as the criteria, the light transmittance with dust particles on the surface was estimated. The result showed that, when the average transmittance decreased to 6.6%, the average number of dust particles was 302. Therefore, it was assumed that 46 particles decreased by 1% of the light transmittance. Thus, at point 13 (the middle of the surface) as an example, with a decrease in the light transmittance from 94 to 88.2%, a 5.8% decrease pertained to 273 dust particles at the point. The average difference between the measured and calculated light transmittance was 3.41%. The average error rate was 5.37%. The accuracy of automatic measurement was verified by manual measurement, and the results were similar to each other (Table 9).

Figure 11. Manual measurement result of light transmittance after 3.5 days of dust deposition.

Table 9. Results of the simulation and measurement of transmittance and the number of dust particles in each section.

	Section 1	**Section 2**	**Section 3**	**Section 4**	**Section 5**
Measured transmittance	88.5	88.8	87.2	87.3	87.6
Simulated number of particles	287	244	300	295	283
Measured number of particles	250	236	309	305	291
Difference (%)	12.87	3.11	3.05	3.26	2.82
	Section 6	**Section 7**	**Section 8**	**Section 9**	**Section 10**
Measured transmittance	85.8	87.6	86.5	87.1	86.8
Simulated number of particles	342	309	311	298	316
Measured number of particles	373	291	341	314	327
Difference (%)	9.01	5.83	9.64	5.27	3.59

Table 9. *Cont.*

	Section 11	Section 12	Section 13	Section 14	Section 15
Measured transmittance	86.8	87.8	88.2	86.3	87.8
Simulated number of particles	328	290	273	331	298
Measured number of particles	327	282	264	350	282
Difference (%)	0.2	2.8	3.41	5.76	5.41
	Section 16	**Section 17**	**Section 18**	**Section 19**	**Section 20**
Measured transmittance	86.9	87.5	86.6	86.8	87.5
Simulated number of particles	317	303	320	314	304
Measured number of particles	323	296	336	327	296
Difference (%)	1.83	2.47	5.14	4.25	2.79
	Section 21	**Section 22**	**Section 23**	**Section 24**	**Section 25**
Measured transmittance	89	86	88	87.6	88.2
Simulated number of particles	267	331	288	299	290
Measured number of particles	227	364	273	291	264
Difference (%)	14.86	9.88	5.28	2.68	9.07

Figure 12 presents the result of the automatic measurement of the light transmittance after 3.5 days of dust accumulation. The slide motor of the automatic measurement platform moved in one direction. Therefore, automatic measurement was conducted only in one direction, and the average light transmittance of the measurement was 86.01%. The light transmittance was 1.38% different from the average light transmittance of 87.39% at 25 measurement points. Therefore, in the future, the results of automatic measurement can be used to represent the transmittance of the solar panel.

Figure 12. Automated measurement result of light transmittance after 3.5 days of dust deposition.

6. Conclusions

Since solar power plants are usually located in open areas such as grasslands and deserts, the surface of the solar panel was prone to dust deposition. Thus, it is important to remove and prevent the deposited dust in solar power generation. Therefore, we studied factors affecting dust deposition on the surface of the solar panel and the relationship between light transmittance and the number of dust particles through calculation based on the weather data and measured transmittance with an automated dust measurement platform. The result showed that dust deposition was effectively predicted considering the wind speed and direction, inclination angles of the solar panel, and time for dust deposition. In Taichung, Taiwan, the northeast wind could remove more dust particles at a wind speed of 5 m/s than the southwest wind. At the wind speed of 1 and 3 m/s, the wind direction did not influence the dust deposition significantly. Wind speed of less than 5 m/s did not affect dust deposition considerably but the wind speed over 5 m/s reduced the dust particles from the surface of the solar panel significantly. The inclination angle also influenced dust deposition when the angle was steeper than 23°. Dust particles tended to gather around the middle part of the surface at this inclination angle. The longer the deposition time, the more particles remained on the surface due to the increased force among the particles and between the particles and the surface of the solar panel. The wind speed of over 5 m/s removed more particles from the surface. The calculated results were compared with the measurement based on transmittance with the proposed dust measurement platform, which showed a difference of only 3.41%. The result of the proposed method in this study provides an important basis for designing the solar power generation plant and decision-making on the maintenance of the solar panel.

Author Contributions: Conceptualization, S.-L.W. and H.-C.C.; Methodology, S.-L.W., H.-C.C. and K.-J.P.; Software, S.-L.W., H.-C.C. and K.-J.P.; Validation, S.-L.W., H.-C.C. and K.-J.P.; Formal analysis, S.-L.W. and H.-C.C.; Data curation, S.-L.W., H.-C.C. and K.-J.P.; Writing—original draft, S.-L.W., H.-C.C. and K.-J.P.; Writing—review & editing, S.-L.W. and H.-C.C. All authors have read and agreed to the published version of the manuscript.

Funding: The study was supported by Ministry of Science and Technology of Republic of China, under Grant No. MOST 111-2221-E-167-005-MY2.

Conflicts of Interest: The authors declare no conflict of interest.

References

1. Ovrum, O.; Marchetti, J.M.; Kelesoglu, S.; Marstein, E.S. Comparative Analysis of Site-Specific Soiling Losses on PV Power Production. *IEEE J. Photovolt.* **2021**, *11*, 158–163. [CrossRef]
2. Fan, S.; Wang, Y.; Cao, S.; Sun, T.; Liu, P. A Novel Method for Analyzing the Effect of Dust Accumulation on Energy Efficiency Loss in Photovoltaic System. *Energy* **2021**, *234*, 121112–121122. [CrossRef]
3. Hammad, B.; Al-Abed, M.; Al-Ghandoor, A.; Al-Sardeah, A.; Al-Bashir, A. Modeling and Analysis of Dust and Temperature Effects on Photovoltaic Systems' Performance and Optimal Cleaning Frequency: Jordan Case Study. *Renew. Sustain. Energy Rev.* **2018**, *82*, 2218–2234. [CrossRef]
4. Ilse, K.; Figgis, B.; Khan, M.Z.; Naumann, V.; Hagendorf, C. Dew as a Detrimental Influencing Factor for Soiling of PV Modules. *IEEE J. Photovolt.* **2019**, *9*, 287–294. [CrossRef]
5. Gholami, A.; Khazaee, I.; Eslami, S. Experimental Investigation of Dust Deposition Effects on Photo-Voltaic Output Performance. *Sol. Energy* **2018**, *159*, 346–352. [CrossRef]
6. Chen, Y.; Wang, D.; Liu, Y.; Dong, Y.; Liu, J. Research on Photovoltaic Performance Reduction Due to Dust Deposition: Modelling and Experimental Approach. *J. Therm. Sci.* **2019**, *6*, 1186–1194. [CrossRef]
7. Saidan, M.; Ghani Albaali, A.; Alasis, E.; Kaldellis, J.K. Experimental Study on the Effect of Dust Deposition on Solar Photovoltaic Panels in Desert Environment. *Renew. Energy* **2016**, *92*, 499–505. [CrossRef]
8. Majeed, R.; Waqas, A.; Sami, H.; Ali, M.; Shahzad, N. Experimental Investigation of Soiling Losses and a Novel Cost-Effective Cleaning System for PV Modules. *Sol. Energy* **2020**, *201*, 298–306. [CrossRef]
9. Klugmann-Radziemska, E.; Rudnicka, M. Decrease in Photovoltaic Module Efficiency Because of the Deposition of Pollutants. *IEEE J. Photovolt.* **2020**, *10*, 1772–1779. [CrossRef]
10. Hertz, H. About the Contact of Solid Elastic Bodies. *J. Pure Appl. Math.* **1881**, *92*, 156–171.
11. Cundall, P.A.; Strack, O.D.L. A Discrete Numerical Model for Granular Assembles. *Geotechnique* **1979**, *29*, 47–65. [CrossRef]
12. Cundall, P. The Measurement and Analysis of Accelerations in Rock Slopes. Ph.D. Thesis, Imperial College London, London, UK, 1971.

13. Huangfu, Y.; Hang, L.; Qin, W.; Shen, C.; Wang, J. Grey Model Simulation Study of Solar Panel Surface Area. *Power Grid Clean Energy* **2016**, *32*, 106–111.
14. *Monthly Report of the Environmental Protection Statistics of the Republic of China*; Environmental Protection Administration of Executive Yuan: Taipei City, Taiwan, 2019; p. 359.
15. Environmental Protection Administration of Executive Yuan. Available online: https://erdb.epa.gov.tw/DataRepository/EnvMonitor/WeatherData.aspx (accessed on 1 April 2018).
16. Feng, Q. The Crushing Performance Analysis and Chamber Optimization of Gyratory Crusher Based on the Discrete Element Method. Master's Thesis, Hunan University, Changsha, China, 2014.
17. Elghannay, H.; Tafti, D.; Kuahai, Y. Evaluation of Physics based Hard-sphere Model with the Soft Sphere Model for Dense Fluid-particle Flow Systems. *Int. J. Multiph. Flow* **2019**, *112*, 100–115. [CrossRef]